Electronic Supplementary Material (ESI) for Journal of Materials Chemistry A.

Supporting Information

ZnO Quantum Dots Anchored in Multilayered and Flexible Amorphous Carbon Sheets for High Performance and Stable Lithium Ion Batteries

Joseph F. S. Fernando,[a] Chao Zhang,[a] Konstantin L. Firestein,[a] Jawahar Y. Nerkar,[b] and Dmitri V. Golberg*[ac]*

[a]*School of Chemistry, Physics and Mechanical Engineering, Science and Engineering Faculty, Queensland University of Technology (QUT), Brisbane, Queensland, 4000, Australia.*

[b]*Institute for Future Environments, Queensland University of Technology (QUT), Brisbane, Queensland, 4000, Australia.*

[c]*International Center for Materials Nanoarchitectonics (MANA), National Institute for Materials Science (NIMS), Namiki 1-1, Tsukuba, Ibaraki 3050044, Japan.*

Corresponding Authors

*E-mail: jf.fernando@qut.edu.au

*E-mail: dmitry.golberg@qut.edu.au

Synthesis of porous ZnO particles

Zinc acetate dihydrate (2.08 g) and ethylene glycol (50 mL) was measured into a round bottom flask. Then the reaction mixture was heated under reflux and held at 70 ºC until all zinc acetate dihydrate was dissolved. Afterwards, the reaction mixture was further heated to 160 ºC and kept at this temperature for 4 hours. The reaction mixture was allowed to cool and the product was separated by centrifugation (9000 RPM, 4 min), washed several times with absolute ethanol and transferred to a drying oven at 60 ºC. The dried powder was used for analysis and battery testing.

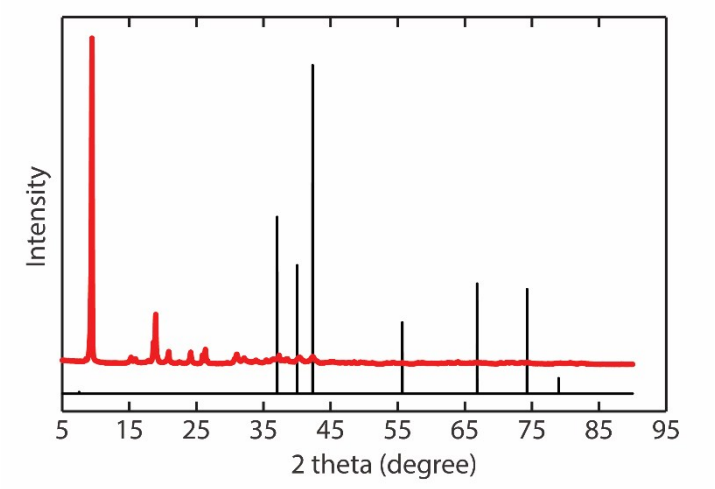

Figure S1: Powder XRD pattern of as prepared zinc glycolate sheets. The line graph shows the diffraction peak positions corresponding to hexagonal wurtzite ZnO powder.

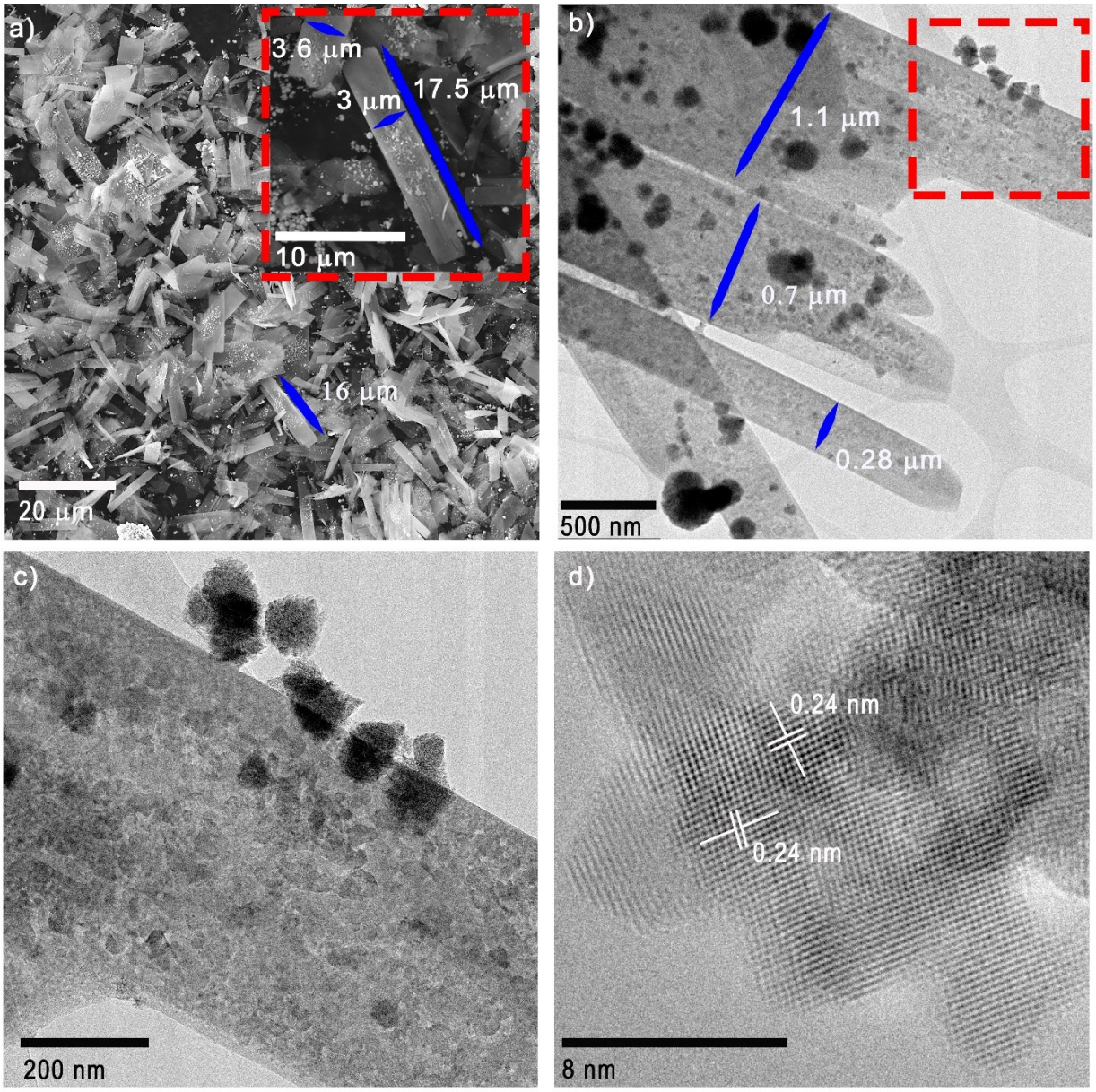

Figure S2: a) SEM (inset shows a high magnification SEM image) and b) TEM image of as obtained zinc glycolate product. c) Magnified TEM image of the area marked in S2b. d) High resolution TEM image of a porous ZnO particle. TEM and SEM imaging revealed that the as synthesized product largely consists of Zn glycolates with sheet-like morphology. ZnGc sheets have mosaic-like surface, their widths are ranging from 0.25 - 5 µm and lengths are up to 20 µm. There are also some porous ZnO nanoparticles sandwiched in between glycolate sheets. High resolution TEM image (S2d**)** of a porous particle reveal lattice fringes with a spacing of 0.24 nm, which can be attributed to (011) planes of wurtzite ZnO.

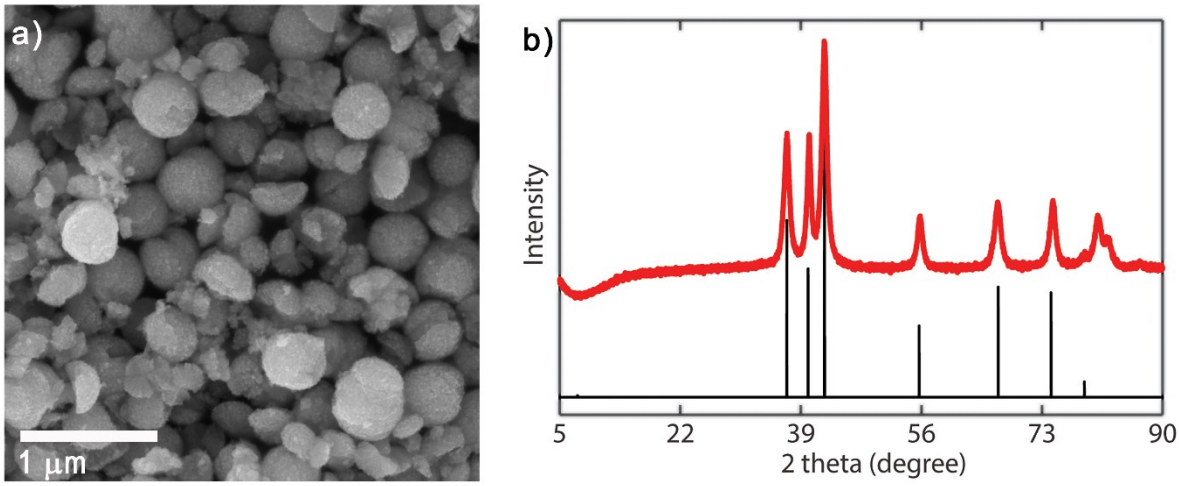

Figure S3: a) SEM image of porous ZnO nanospheres formed when oleylamine was omitted from the reaction system. b) XRD pattern of ZnO nanospheres, which conforms to hexagonal wurtzite crystal structure of ZnO.

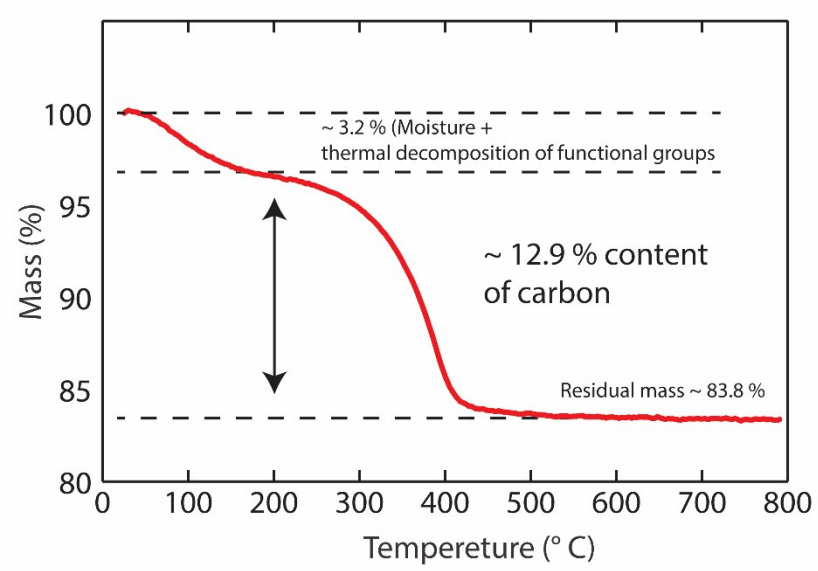

Figure S4: TGA curve for ZnO-QDs@CMS. TGA experiment was carried out in air from 25 °C to 800 °C at a heating rate of 5 °C/min. The initial weight loss of ~ 3.2 % could be attributed to adsorbed moisture loss and thermal decomposition of functional groups.[1]

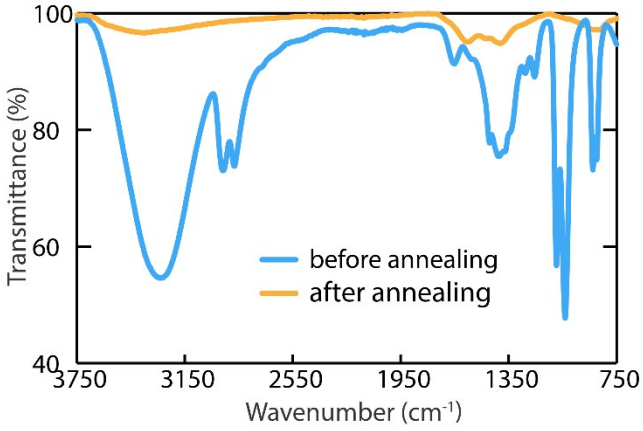

Figure S5: FTIR spectra obtained before and after the annealing of Zn glycolate precursor complex under an Ar environment at 350 °C for 30 min.

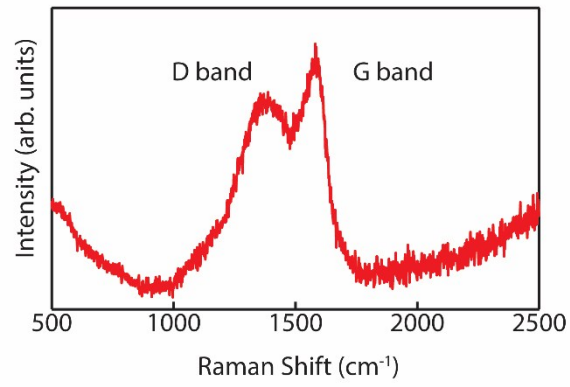

Figure S6: Raman spectrum obtained from a ZnQ-QDs@CMS sample, showing D and G bands corresponding to amorphous carbon or disordered graphite.

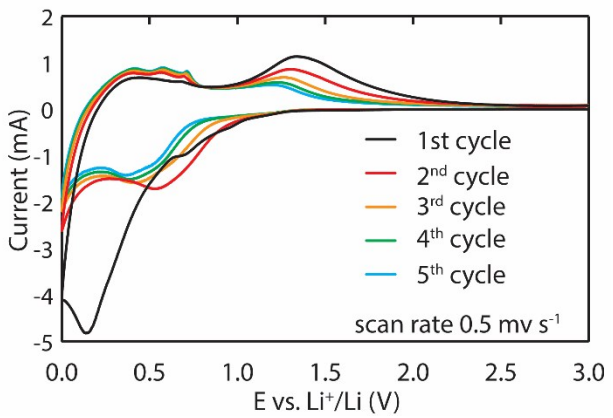

Figure S7: Cyclic voltammetry for pristine ZnO particles conducted in a potential range of 0.0 to 3.0 V for five cyclic sweeps (scan rate: 0.5 mV s^{-1})

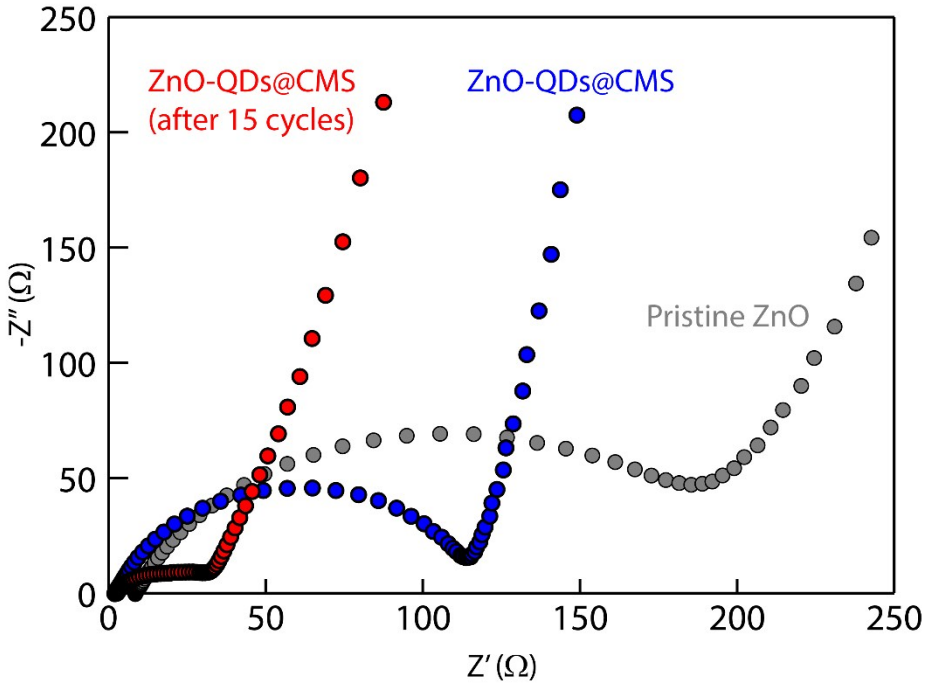

Figure S8: Impedance spectra of Pristine ZnO and ZnO-QDs@CMS anode materials.

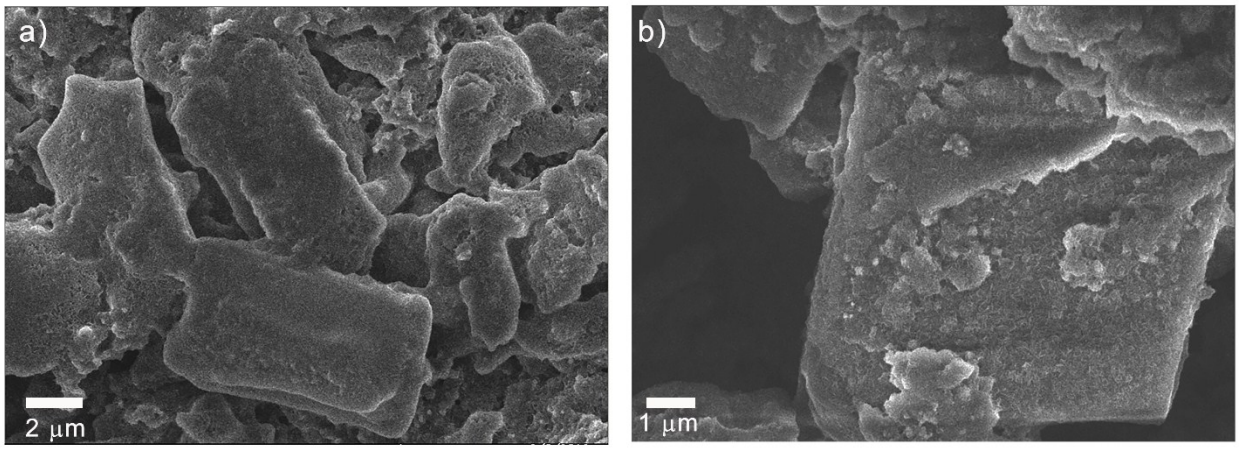

Figure S9: SEM images of a ZnO-QDs@CMS electrode material after performing 100 charge/discharge cycles at a specific current of 50 mA g^{-1}.

Table S1: Comparison of performance of the ZnO QDs@CMS anode material to recently reported novel ZnO QD/C based composite materials.

Material*	**Reversible Capacity (mAh g^{-1})**	**Current Density (mA g^{-1})**	**Cycle number**
ZnO@ZnO QDs/C NRAs[2]	699	500	100
ZnO QDs@porous carbon (550N)[3]	1150	75	50
Amorphous ZnO QDs/MPCBs[1]	930 510	100 1000	85 400
ZnO QD/Graphene[4]	540 400	100 1000	100
This work: ZnO-QDs@CMS	1015 943 565	50 100 1000	80 132 350

***Refer the recent review paper by Duan *et al.*[5] for a comprehensive table on various Zn- and ZnO-based anode materials for lithium ion batteries.**

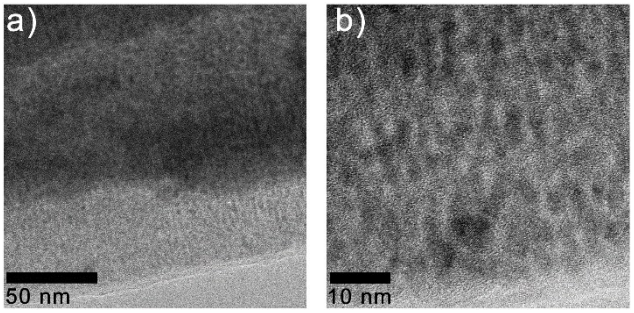

Figure S10: (a,b) High magnification TEM images of ZnO-QDs@CMS captured after the 4th *in situ* TEM lithiation, confirming that ZnO-based composite material maintained the integrity of the structure during (de)lithiation.

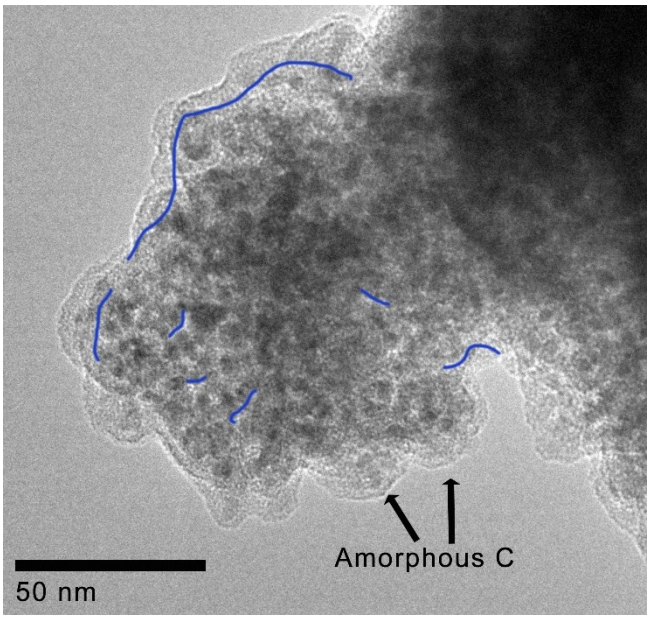

Figure S11: TEM image of an isolated carbon-wrapped mesoporous ZnO particle (C-ZnO).

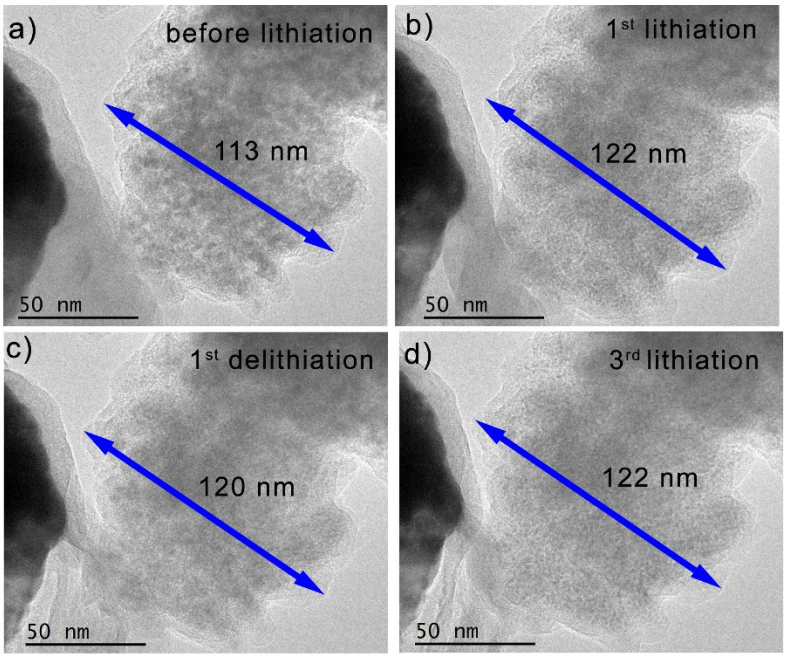

Figure S12: TEM images of an isolated mesoporous C-ZnO particle. a) Before lithiation, b) After first lithiation, c) After first delithiation and d) After third lithiation. *In situ* TEM experiment on the isolated C-ZnO particle showed that volume expansion after the first lithiation is ~ 22 %, which is less than what was observed for the pristine porous ZnO (~ 30 %). More importantly, formation of dark nanocrystals or Zn grains was not observed even after the 3rd cycle.

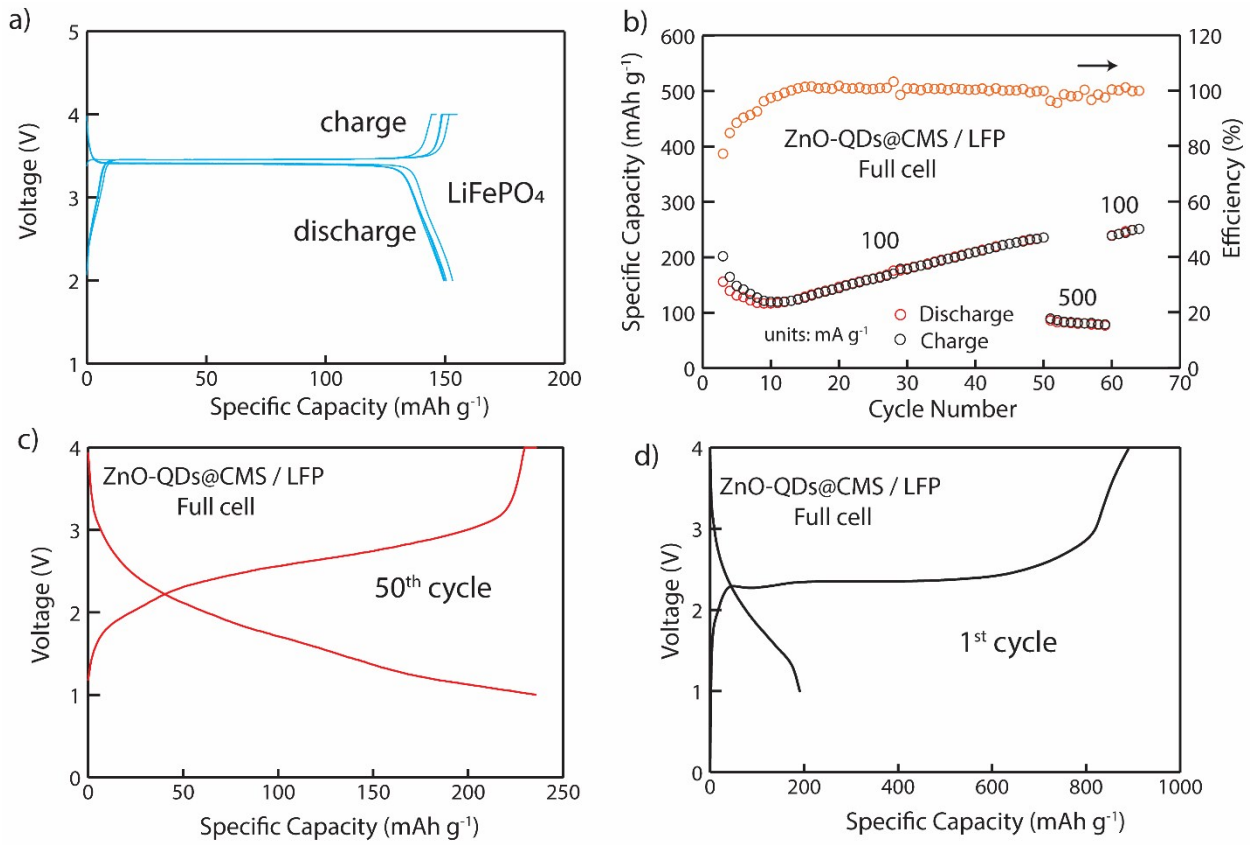

Figure S13: a) Voltage profile of LFP cathode at 50 mA g^{-1}, b) Cycling performance of a ZnO-QDs@CMS/LFP full-cell (2nd cycle onwards), c) Voltage profile for the 50th cycle of the full cell and d) Voltage profile for the 1st cycle of the full cell.

References

1. Z. Tu, G. Yang, H. Song and C. Wang, *ACS Appl. Mater. Interfaces*, 2017, **9**, 439-446.
2. G. Zhang, S. Hou, H. Zhang, W. Zeng, F. Yan, C. C. Li and H. Duan, *Adv. Mater.*, 2015, **27**, 2400-2405.
3. S. J. Yang, S. Nam, T. Kim, J. H. Im, H. Jung, J. H. Kang, S. Wi, B. Park and C. R. Park, *J. Am. Chem. Soc.*, 2013, **135**, 7394-7397.
4. X. Sun, C. Zhou, M. Xie, H. Sun, T. Hu, F. Lu, S. M. Scott, S. M. George and J. Lian, *J. Mater. Chem. A*, 2014, **2**, 7319-7326.
5. L. Wang, G. Zhang, Q. Liu and H. Duan, *Mater. Chem. Front.*, 2018, **2**, 1414-1435.